Nuclear Engineering and Technology 52 (2020) 964–974

Contents lists available at ScienceDirect

Nuclear Engineering and Technology

journal homepage: www.elsevier.com/locate/net

Original Article

Indefinite sustainability of passive residual heat removal system of small modular reactor using dry air cooling tower

Min Wook Na [a], Doyoung Shin [a], Jae Hyung Park [a], Jeong Ik Lee [c], Sung Joong Kim [a, b, *]

[a] Department of Nuclear Engineering, Hanyang University, 222 Wangsimni-ro, Seongdong-gu, Seoul 04763, Republic of Korea
[b] Institute of Nano Science & Technology, Hanyang University, 222 Wangsimni-ro, Seongdong-gu, Seoul 04763, Republic of Korea
[c] Department of Nuclear and Quantum Engineering, Korea Advanced Institute of Science and Technology, 291 Daehak-ro, Yuseong-gu, Daejeon 34141, Republic of Korea

ARTICLE INFO

Article history:
Received 8 July 2019
Received in revised form
15 October 2019
Accepted 4 November 2019
Available online 6 November 2019

Keywords:
Passive residual heat removal system
dry air cooling tower
Small modular reactor
Emergency cooling sustainability
Grace period
MARS-KS

ABSTRACT

The small modular reactors (SMRs) of the integrated pressurized water reactor (IPWR) type have been widely developed owing to their enhanced safety features. The SMR-IPWR adopts passive residual heat removal system (PRHRS) to extract residual heat from the core. Because the PRHRS removes the residual heat using the latent heat of the water stored in the emergency cooldown tank, the PRHRS gradually loses its cooling capacity after the stored water is depleted. A quick restoration of the power supply is expected infeasible under station blackout accident condition, so an advanced PRHRS is needed to ensure an extended grace period. In this study, an advanced design is proposed to indirectly incorporate a dry air cooling tower to the PRHRS through an intermediate loop called indefinite PRHRS. The feasibility of the indefinite PRHRS was assessed through a long-term transient simulation using the MARS-KS code. The indefinite PRHRS is expected to remove the residual heat without depleting the stored water. The effect of the environmental temperature on the indefinite PRHRS was confirmed by parametric analysis using comparative simulations with different environmental temperatures.

1. Introduction

Small modular reactors (SMRs) have attracted worldwide attention as a practical option for satisfying the increasing energy demand [1,2]. Many countries with advanced nuclear technologies have been developing SMRs such as the NuScale, mPower, System-integrated Modular Advanced Reactor (SMART), International Reactor Innovative and Secure (IRIS), Autonomous transportable on-demand reactor module (ATOM), and Central Argentina de Elementos Modulares (CAREM) [3–8], to mention a few. These SMRs share the common characteristics of being integrated with a pressurized water reactor (IPWR). While the IPWR-type SMR (hereafter called SMR-IPWR) has the same configuration as commercial PWR-type nuclear power plants (NPPs), it has distinctively different primary systems [9]. In the IPWR design, the major components of the primary system, such as the reactor core, steam generators (SGs), and pumps, are installed inside the reactor vessel [10].

The SMR-IPWR exhibits more enhanced safety compared with large reactors. Owing to its simplified design eliminating large pipes, the SMR-IPWR reduces the possibility of the loss of coolant accident (LOCA), which is a representative design basis accident (DBA). The SMR-IPWR also adopts passive safety systems (PSS) to reinforce the capability of mitigating beyond design-basis accidents, such as station blackout (SBO) accidents. To eliminate the need for electrical power, PSS are designed to ensure reactor safety by means of naturally driven forces, such as gravity or pressure differences. Additionally, PSS have been researched to enhance safety and reduce the design complexity [11]. Previous studies have particularly pointed out that sufficient height is required for adopting a PSS that uses the gravity force to drive the natural circulation flow. The arrangement of the primary system in the SMR-IPWR provides suitable conditions to gravity-driven PSS by ensuring a sufficient height difference [12]. Thus, the PSS can play a significant role in ensuring the safety of the SMR-IPWR [13].

From the viewpoint of NPP accident management, the most critical consideration is to completely remove the residual heat generated from the core after shutdown. In this respect, many studies have been conducted to develop the PSS, which exports

* Corresponding author.Department of Nuclear Engineering, Hanyang University. South Korea.
E-mail address: sungjkim@hanyang.ac.kr (S.J. Kim).

https://doi.org/10.1016/j.net.2019.11.003

Abbreviation

ATOM	Autonomous transportable on-demand reactor module
DACT	Dry air cooling tower
DBA	Design basis accident
ECT	Emergency cooldown tank
HS	Heat structure
HX-DACT	Heat exchanger in dry air cooling tower
HX-ECT	Heat exchanger in ECT connected with PRHRS loop
HX-IL	Heat exchanger in ECT connected with intermediate loop
IPWR	Integrated pressurized water reactor
IRIS	International reactor innovative and secure
KAERI	Korea Atomic Energy Research Institute
LMTD	Logarithmic mean temperature difference
LOCA	Loss of coolant accident
MARS-KS	Multi-dimensional analysis of reactor safety
NPP	Nuclear power plant
PD	Pressure drop
PRHRS	Passive residual heat removal system
PSS	Passive safety system
SMR	Small modular reactor
SBO	Station blackout
SMART	System-integrated modular advanced reactor
SG	Steam generator
SJ	Single junction
SV	Single volume
TMJ	Time dependent junction
TDV	Time dependent volume
USNRC	United States Nuclear Regulatory Commission

Nomenclature

C_p	Specific heat [J/kg°C]
D	Tube diameter [m]
F	Reynolds number factor [−]
f	Darcy friction factor [−]
g	Gravitational constant [m/s^2]
H	Length of thermal center [m]
h_{fg}	Latent heat of vaporization [J/kg]
k_f	Fluid thermal conductivity [W/m°C]
L	Tube length [m]
P	Pressure [N/m^2]
ΔP	Difference between saturation pressure based on T_w and total pressure [N/m^2]
ΔP_{acc}	Pressure drop by acceleration [N/m^2]
ΔP_{form}	Pressure drop by form [N/m^2]
ΔP_{fric}	Pressure drop by friction [N/m^2]
Pr	Prandtl number [−]
P/D	Pitch to diameter ratio [−]
R	Thermal resistance [°C/W]
Ra	Rayleigh number [−]
Re	Reynolds number [−]
S	Suppression factor [−]
T_{sat}	Saturation temperature [°C]
T_w	Wall temperature [°C]
ΔT_w	Difference between T_w and T_{sat} [°C]
U	Overall heat transfer coefficient [W/m^2°K]

Greek letters

μ_f	Fluid viscosity [kg/m·s]
ρ_f	Fluid density [kg/m^3]
ρ_g	Vapor density [kg/m^3]
σ	Vapor-liquid surface tension [N/m]

residual heat to cool down the core; this is called a passive residual heat removal system (PRHRS). The PRHRS transfers residual heat to the emergency cooldown tank (ECT) through a naturally circulating flow. The transferred residual heat is removed by the sensible and latent heat of the water stored in the ECT. The feasibility of the PRHRS has been evaluated by many studies. Bae et al. proposed a PRHRS design for a SMART developed by the Korea Atomic Energy Research Institute (KAERI) [4]. Park et al. confirmed performance sensitivity of the PRHRS using an integrated test facility [14]. Min et al. have experimentally verified the performance of the PRHRS for SMART [15]. Zhang et al. confirmed that the PRHRS effectively removed decay heat from the core of CPR1000 by establishing stable natural circulation [16]. Transient simulations for 3000 s using RELAP5/MOD3.4 have been conducted to investigate the cooling capability of the PRHRS. Wang et al. have also investigated the transient characteristics of the PRHRS, confirmed the sufficient cooling capacity of the PRHRS, and proposed optimal design parameters [17]. Xia et al. assessed the feasibility of the PRHRS for SMR-IPWR (220 MWe) by conducting a simulation for 3000 s using RELAP5 [12]. Thus, previous studies have verified the capability of the PRHRS to cool down the reactor core in the early stages of accidents.

Although the cooling capability of the PRHRS has been verified by many studies, the PRHRS has a critical limitation. Because the PRHRS uses the latent heat of the water stored inside the ECT, the PRHRS inevitably loses its cooling capability when the stored water is depleted. Consequently, the cooling sustainability of the PRHRS is determined by the storage capacity of the ECT. Because the volume of the ECT cannot be increased infinitely, the cooling sustainability of the PRHRS should be evaluated by considering sufficient time for the recovery of the power supply system. In the event of SBO, the quick restoration of the power supply is essential for successfully removing the residual heat. However, it was confirmed from the Fukushima accident in 2011, that it is difficult to recover the power supply as quickly as planned in the event of the accidents owing to the destruction of infrastructure [18]. If the recovery of the power supply is delayed beyond the cooling sustainability of the PRHRS, a severe accident may occur. Thus, an advanced PRHRS concept is needed to ensure the long-term safety of NPPs, even without the quick restoration of the power supply [19].

To extend the sustainability of the PRHRS, the coolant used as an ultimate heat sink must remain without any power supply for as long as possible. The only coolant satisfying this requirement is air, which does not need to be stored because, unlike water, it can be supplied without being depleted. Many researchers have used air as the ultimate heat sink to investigate various design concepts with regard to the PRHRS. First, Zhang et al. proposed a design for the air-cooled PRHRS, which directly removes the residual heat with air, instead of water, by replacing the ECT with the dry air cooling tower (DACT), as shown in Fig. 1(a) [20]. However, Wang et al. conducted comparative simulations and confirmed that the air-cooled PRHRS is less effective in the early stages of an accident, compared with the conventional water-cooled PRHRS [21]. Secondly, Kim et al. proposed a new design by adopting the DACT to condense the steam generated in the ECT [22]. By returning the condensed water back to the ECT through the closed system, the boiling loss of the water in the ECT was prevented, as shown in Fig. 1(b). Because, in this design, steam circulates through the closed system, it is required

that the DACT always has sufficient cooling capacity to condense all steam generated from the ECT. However, the cooling capability of the DACT greatly varies depending on the environmental temperature. If the DACT fails to completely condense the steam, the ECT can be pressurized and this may affect the integrity of the entire system. The last approach is to indirectly couple the DACT with the PRHRS using an additional intermediate loop, as shown in Fig. 1(c). Lv et al. assessed the cooling capability of the new PRHRS and confirmed the effects of the design variables up to 10,000 s after reactor shutdown [23]. Moreover, they demonstrated that the cooling performance of the DACT does not affect the cooling capability of the PRHRS. Nevertheless, because the simulations were conducted in the early stage after the SBO accident, the long-term cooling effect of adopting the DACT to extend the sustainability of the PRHRS was not confirmed.

This paper proposes the improved design concept of an indefinite PRHRS for the SMR-IPWR by indirectly coupling the DACT with the conventional PRHRS. By utilizing the conventional PRHRS, whose cooling capability has already been verified, the residual heat can be reliably removed in the early stages of an accident. The DACT removes heat from the ECT through additional intermediate loops and thus contributes to the extension of the cooling sustainability of the PRHRS. If the DACT removes more heat than the generated residual heat, an indefinite grace period can be guaranteed. Thus, the objectives of this study are to confirm the feasibility of the indefinite PRHRS and evaluate the effect of environmental conditions on the sustainability of the indefinite PRHRS. By conducting a transient simulation for 72 h, the long-term cooling performance of the indefinite PRHRS was successfully assessed for the first time. Moreover, parametric analyses were conducted to confirm the effect of the environmental temperature on the grace period. The best thermal-hydraulic system analysis code, namely, the multi-dimensional analysis of reactor safety (MARS-KS) code based on RELAP5 and developed in the Republic of Korea, was used to carry out transient analysis for the entire system.

2. SMR-IPWR with indefinite PRHRS

2.1. Design of SMR-IPWR

An IPWR that generates 330 MW of thermal power under normal operation, namely, the SMR-IPWR, was selected as the reference reactor. Because the configuration of this reactor is similar to the configuration of the PWR-type reactor, the major operating conditions of the primary coolant are similar to those of general PWRs, as presented in Table 1. To install the major components of the primary system in the reactor vessel, the SMR-IPWR adopts a helical tube for integrated SGs. With these compact helical-type SGs, it is possible to install four SGs in the limited volume of the reactor vessel.

2.2. Description of indefinite PRHRS

The schematic diagram of the indefinite PRHRS concept for the SMR-IPWR is shown in Fig. 2. During normal operation, the phase change of the feed water in the SGs occurs through a boiling process. The steam from the SGs flows to the turbine following the main steam line for the generation of electrical power. The condenser condenses the exhausted steam after the turbine operation. Finally, the condensed feed water flows back to the SGs. If SBO occurs, the feed water flows into the other path. After reactor shutdown, the primary coolant heated by the residual heat flows to the SGs. Simultaneously, the circulation of the feed water through the turbine and condenser is stopped, and the PRHRS valve is opened. The PRHRS valve diverts the steam path from the main steam line to the PRHRS loop.

The steam goes up to the heat exchanger (HX) in the ECT (HX-ECT) through the PRHRS loop and is cooled down in the HX-ECT by the latent heat of the water stored in the ECT. The HX-ECT is composed of the vertical tube bundles to reduce the resistance of the natural circulation and to secure sufficient heat transfer area. Because SG and ECT act as a heat source and heat sink, respectively, natural circulation flow is established. By relying on natural circulation, PRHRS removes the residual heat without an electrical power supply.

Because the cooling sustainability of the PRHRS primarily depends on the inventory of the water stored in the ECT, it is important to maintain the amount of water stored in the ECT. To mitigate the loss of stored water, another HX in the ECT (HX-IL), intermediate loop, and DACT are designed for installation. Through the intermediate loop, the heat from the stored water of the ECT is transferred to the DACT, wherein the air is heated by the HX in the DACT (HX-DACT) and rises through the channels. The vertical tube bundles composing the HX-DACT are installed at the bottom of the DACT. To compensate low heat transfer capability of air, the tubes in the HX-DACT are equipped with fins to enlarge heat transfer area. As shown in Fig. 2, the fins are attached parallel to the tube to reduce resistance of the vertical air flow. As the environmental air naturally flows into the DACT, owing to the ascent of air inside the DACT, the DACT can continuously remove heat. For heat removal through the DACT, the grace period provided by the PRHRS can be extended. Moreover, if the heat removed by the DACT is equal to the

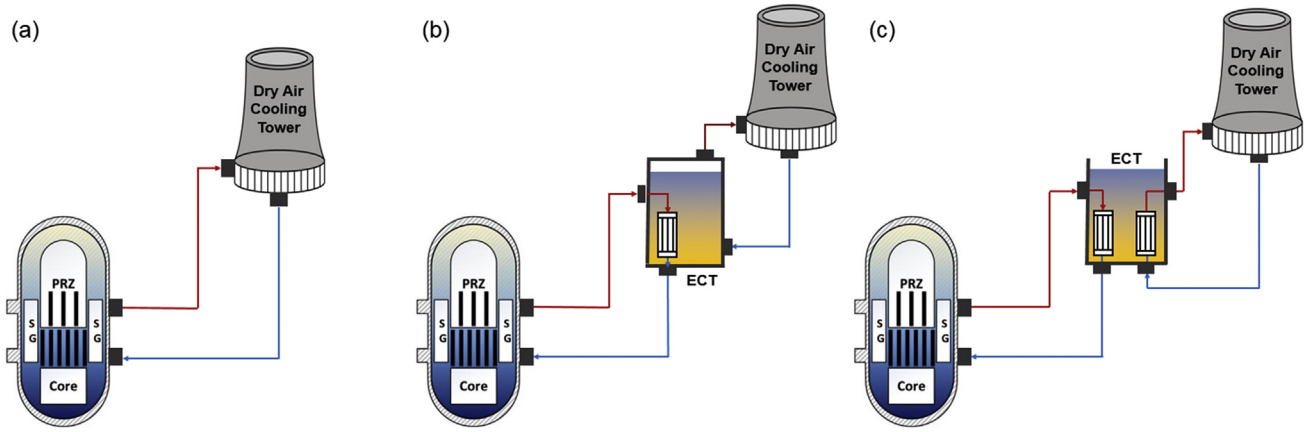

Fig. 1. (a) Air-cooled PRHRS by replacing ECT with DACT; (b) design of PRHRS directly coupled with DACT; (c) design of PRHRS indirectly coupled with DACT.

residual heat transferred to the ECT, it is possible to ensure an indefinite grace period by maintaining the water level of the ECT. The advanced concept of a PRHRS indirectly coupled with a DACT to achieve indefinite cooling sustainability is called indefinite PRHRS.

2.3. Design calculation of indefinite PRHRS

The major design parameters of the indefinite PRHRS were determined through design calculations using MATLAB code. The primary objective of the DACT is to extract most of the residual heat from the ECT to prevent the loss of stored water by boiling. The design parameters for the major components of the indefinite PRHRS, such as the ECT, intermediate loop, and DACT, were determined from the calculation result.

The indefinite PRHRS is a safety system operating under transient conditions, such as accident situations. However, analytic design calculations can be conducted under steady-state conditions. Hence, appropriate assumptions must be made and certain conditions are required. The condition applied to the design calculation is the time point when the water stored in the ECT maintains saturation. When the stored water is at a state of saturation, the water also maintains a saturation temperature. Because the temperature of the stored water is fixed at the saturation temperature, the steady-state design calculation is possible. Additionally, the environmental temperature and saturation temperature are assumed to be fixed at 20 °C and 100 °C, respectively.

To calculate the amount of heat transfer in the HXs, a logarithmic mean temperature difference (LMTD) method was used, as expressed by Equations (1)–(3) [24,25]. At the HX-IL, which is a co-current flow type, ΔT_A is the temperature difference between the inlet of the hot and cold sides. ΔT_B also indicates a temperature difference between the outlet of the hot and cold sides. At the HX-DACT, which is a counter-current flow type, ΔT_A is the temperature difference between the inlet of the hot side and the outlet of the cold side. ΔT_B is the temperature difference between the outlet of the hot side and the inlet of the cold sides. U is an overall heat transfer coefficient and A indicates the total heat transfer area. $U{\cdot}A$ is calculated by the thermal resistance analogy. The total thermal resistance is calculated by summing the thermal resistances of water convection and conduction through the tube thickness and air convection, respectively.

$$LMTD = \frac{\Delta T_A - \Delta T_B}{\ln \Delta T_A - \ln \Delta T_B} \tag{1}$$

$$Q = \mathrm{U}\cdot\mathrm{A}\cdot\mathrm{LMTD} \tag{2}$$

Table 1
Major parameters of SMR-IPWR.

Design Parameters	Value
Reactor Core	
Reactor type	Integrated PWR
Thermal power (MWt)	330
Electrical power (MWe)	100
Fuel material	UO2
Fuel assembly	17 × 17
Operating pressure (MPa)	15
Core inlet temperature (K)	546
Core outlet temperature (K)	588
Core mass flow rate (kg/s)	1428.5
Steam Generator	
SG type	Helical tube
SG pressure (MPa)	4.42
Tube length (m)	14.4
Tube number	990 × 4

$$\mathrm{U}\cdot\mathrm{A} = \frac{1}{R_{convection,water} + R_{conduction} + R_{convection,air}} \tag{3}$$

The natural circulation flows established in the intermediate loop and DACT are calculated using Equation (4) [23]. The natural circulation flow is determined when the natural draft pressure driven by the density difference offsets the total pressure drop. The natural draft pressure and total pressure drop can be calculated by using left and right sides of Eq. (4), respectively. In Eq. (4), H is a length of thermal center, which indicates a height difference between heat source and heat sink. The total pressure drop is the sum of the pressure drop caused by friction, acceleration, and form loss. Each pressure drops are calculated through Eq. (5) to (8), respectively. The pressure drop due to the sudden expansion (SE) and contraction (SC) calculated by Eq. (7) and (8) are the pressure drops by form loss [26]. L, D, f, ρ, v, and A from Eq. (5) to (8) are tube length, tube diameter, Darcy friction factor, density, velocity, and flow area, respectively. The subscript number 1 and 2 in Eq. (6) to (8) represent the state of the region before and after the acceleration, sudden expansion, and contraction, respectively.

$$(\rho_{cold} - \rho_{hot}) \cdot g \cdot H = \Delta P_{fric} + \Delta P_{acc} + \Delta P_{form} \tag{4}$$

$$\Delta P_{fric} = f\frac{L}{D}\frac{\rho v^2}{2} \tag{5}$$

$$\Delta P_{acc} = \rho_2 v_2^2 - \rho_1 v_1^2 \tag{6}$$

$$\Delta P_{SE} = \frac{1}{2}\rho\left(1 - \frac{A_2}{A_1}\right)^2 v_2^2 \tag{7}$$

$$\Delta P_{SC} = 0.06\rho v_2^2 \tag{8}$$

Fig. 3 shows the overall calculation algorithm of the MATLAB code. First, the calculation to determine major variables of the intermediate loop was conducted. The temperatures in the hot and cold side of the intermediate loop were initially assumed and the mass flow rate (MFR_w) in intermediate loop was estimated by using Eq. (4). The mass flow rate was estimated when the natural draft pressure (P_{draft}) driven by the density difference offsets the total pressure drop (ΔP_{total}). The P_{draft} and ΔP_{total} were calculated by using left and right sides of Eq. (4). The transferred heat at HX-IL could be calculated by using estimated mass flow rate and LMTD method through Eq. (1) to (3). The transferred heat at HX-IL was compared with Q_1, which is the heat transferred by water inside the intermediate loop. Until both values of transferred heat at the HX-IL and intermediate loop were balanced, the calculation was iteratively conducted with elevating temperature in the hot side of the intermediate loop. In the next procedure, the calculation for DACT was initiated by assuming hot air temperature in the DACT. Following the similar process, the mass flow rate of air (MFR_{air}) was determined when heat transferred at the HX-DACT was balanced with the heat transferred by air (Q_2) inside the DACT. As the final process, the iterative calculation was conducted with elevating temperature in the cold side of the intermediate loop until the values of transferred heat at HX-IL and HX-DACT were balanced. Through this process, the heat transfer capability of the DACT in certain design values was determined. The design values capable of removing most of the residual heat from the ECT were selected as the reference design parameters in this study, as summarized in Table 2. In addition, the major parameters of vertical tube bundle type heat exchanger (i.e. HX-ECT, HX-IL, and HX-DACT) were also shown.

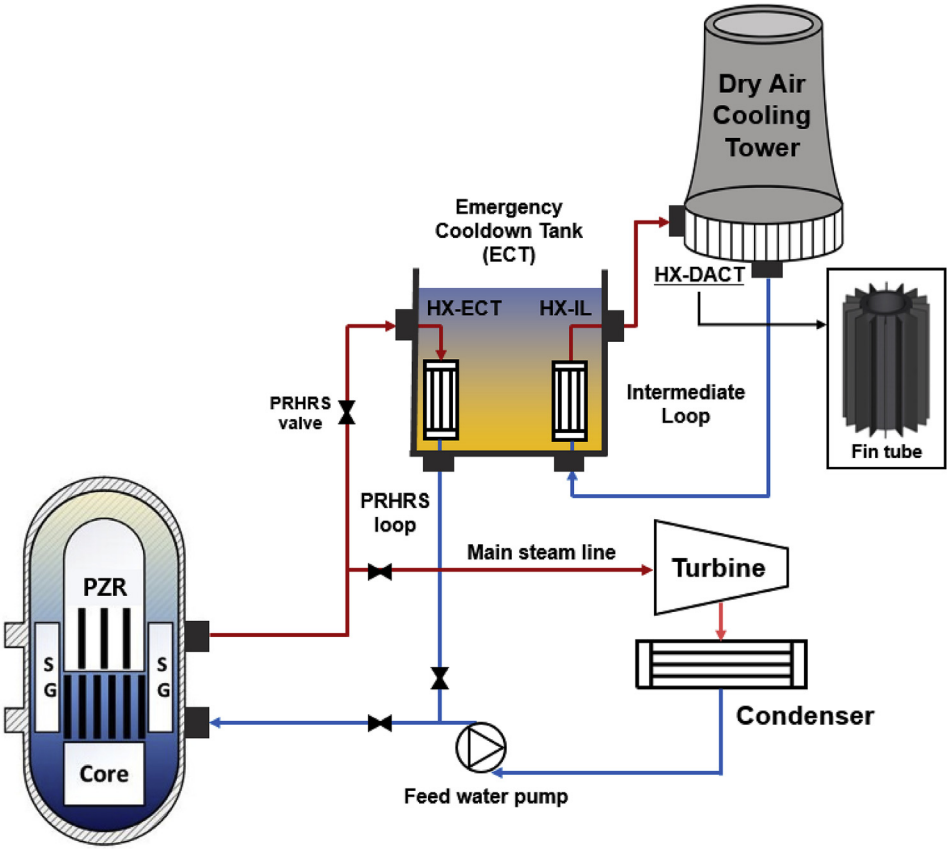

Fig. 2. Schematic diagram of indefinite PRHRS at SMR-IPWR.

3. MARS-KS model of SMR-IPWR with indefinite PRHRS

The MARS-KS code was used to investigate the behavior of the reactor and that of the indefinite PRHRS. Moreover, MARS-KS has been widely used for the thermal-hydraulic analysis of light water reactor systems because it is the best estimation code developed in the Republic of Korea [27,28]. This code was developed by the KAERI to conduct multi-dimensional thermal-hydraulic system analysis by consolidating two codes, RELAP5/MOD3.2 and COBRA-TF, developed by the United States Nuclear Regulatory Commission (USNRC) [29]. RELAP5/MOD3.2 and COBRA-TF were merged into the MARS for one-dimensional (1D) system analysis modules and three-dimensional (3D) vessel analysis modules, respectively. In this study, the 1D system analysis modules of MARS were used to conduct the transient system analysis of the SMR-IPWR with the indefinite PRHRS. The 1D modules of MARS are based on a two-fluid model for two phase flows, similar to RELAP5.

For transient analysis at the system scale, the 1D MARS-KS model of the SMR-IPWR with indefinite PRHRS has been developed. In their entirety, the systems were constructed using hydrodynamic components such as pipes, time dependent volume (TDV), single volume (SV), time dependent junction (TDJ), and single junction (SJ) [30]. Using these hydrodynamic components, we defined the geometric structure and major conditions of each fluid. Heat transfer phenomena, such as conduction, convection, and condensation, were modelled by the heat structure (HS) in the 1D modules of the MARS. The HS is used for modelling the heat generation, heat transfer between the physical structure and ambient fluid, and heat transfer between the two fluids.

Fig. 4 shows the 1D MARS-KS model of the SMR-IPWR with the indefinite PRHRS. The primary and secondary systems of the SMR-IPWR are presented in Fig. 4(a). The pipe components 200 and 210 represent the two channels of the reactor core. The HS connected with the P200 and P210, respectively, simulates the heat generated by the reactor core. The primary coolants flowing through the four SGs are modelled as P131, P132, P133, and P134. The feed water flows through the other side of the SGs are also modelled as P430, P530, P630, and P730. The heat transfer between the primary coolant and the secondary feed water is simulated by the HSs connecting both side pipes. The turbine and condenser, which do not have a significant impact on accident analysis, are simply replaced with the TDV and TDJ components in the MARS code. TMV980 simulates the supply of feed water to the SGs during normal operation, and the supply of feed water stops after reactor shutdown. TMV801 simulates an outlet of the feed water to replace the main steam line. The MARS model of the indefinite PRHRS is shown in Fig. 4(b), and comprises four PRHRS loops, two ECTs, two intermediate loops, and the DACT. The four PRHRS loops allocated to each SG are divided into two groups and are connected with the two ECTs. Valves 485, 585, 685, and 785 are equipped at each PRHRS loop to operate the PRHRS at reactor shutdown. The ECT is modelled with two pipe components connected by a multi-junction. The method for modelling a large pool such as the ECT is commonly used to simulate the lateral flow and water mixing in 1D system code [31,32]. Sets P850-860 and P870-865 were modelled to simulate the two ECTs. Each ECT has an intermediate loop for transferring heat to the DACT. P895 and P925 represent the heat exchanger installed at the bottom side of the DACT at the same elevation. The DACT is comprised of two pipes 950 and 955. TMV940 and TMV960 represent the environmental air in the vicinity of the inlet and outlet of the DACT, respectively.

The HS 475, 575, 675, 775 and HS 880, 910 simulate the heat

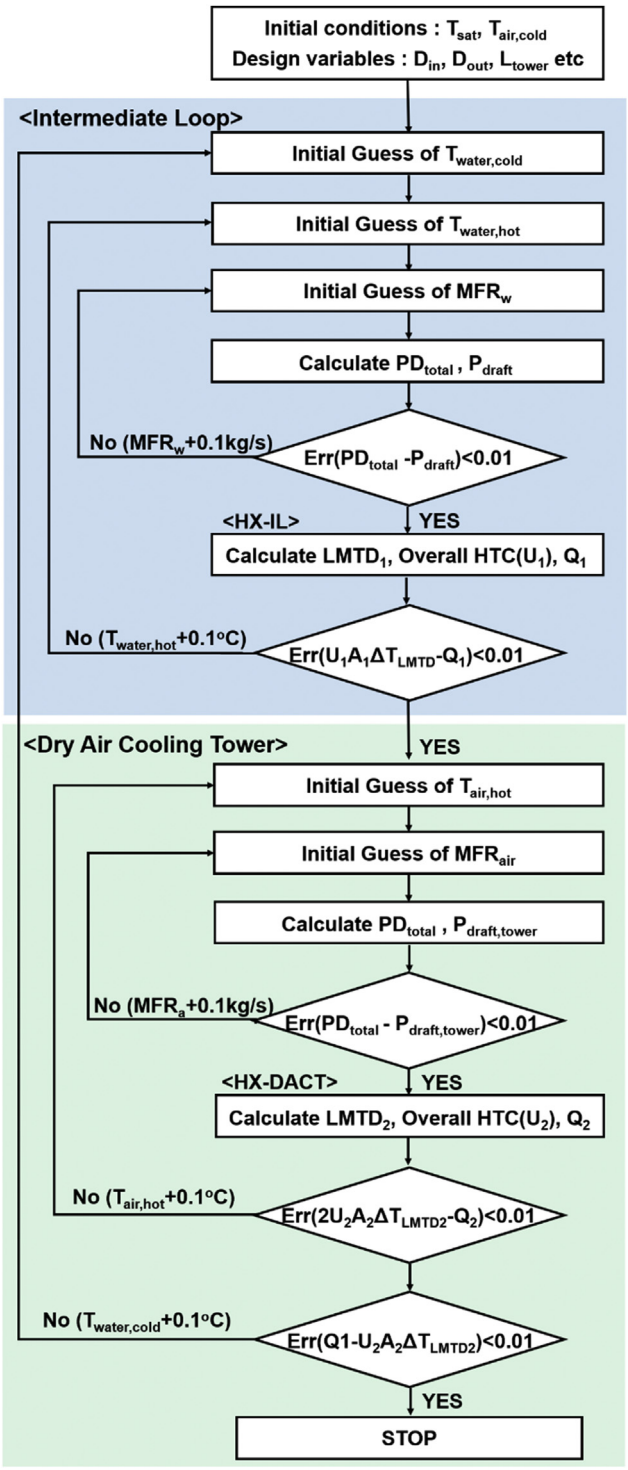

Fig. 3. Algorithm for analytic calculations using MATLAB code.

transfer at the HX-ECTs and HX-IL using the heat transfer correlations considered in the MARS code [26]. Depending on the state of the water stored in the ECT, they simulate diverse heat transfer phenomena such as convection and boiling heat transfer. Before the temperature of the stored water reaches the point of saturation, they simulate the convection heat transfer using Equation (9) and (10) [33]. Eq. (9) developed by Inayatov is the more suitable model for the convective heat transfer at the tube bundles geometry [34]. This model based on the Dittus-Boelter correlation, which is the default model of the MARS-KS, considers the tube bundle effect on the convective heat transfer. For the tube bundle effect, the pitch-to-diameter ratio (P/D) is used as a multiplier factor. The default value of 1.1 was utilized as the pitch-to-diameter ratio of the heat exchangers in this study. After the stored water starts to boil, Equation (11) is used to simulate the saturated boiling heat transfer phenomena. Chen analyzed the boiling heat transfer using two mechanisms: the ordinary macro-convective mechanism by the fluid and the micro-convective mechanism by the bubble [35]. The h_{mac} and h_{mic} are calculated by using Eq. (12) and (13), respectively. The h_{mac} is equivalent to the convective heat transfer coefficient calculated by Eq. (9), with which the bundle effect is considered. F and S in Eq. (11) are Reynolds number factor and suppression factor, respectively, which are determined empirically.

The heat transfer at the HX-DACT are also modelled by the HS 895 and 925. They simulate the convection of water and air at the inside and outside of the HX-DACT, respectively. The Dittus-Boelter model was used to calculate the heat transfer coefficient of water inside the tubes [36] while that of the outside of the HX-DACT was calculated by Equation (9) to consider bundle effect.

$$\mathrm{Nu} = \frac{hD}{k} = CRe^{0.8}Pr^{0.4} \quad with \;\; C = 0.023\frac{P}{D} \tag{9}$$

$$\mathrm{Nu} = \left\{ 0.825 + \frac{0.387Ra^{\frac{1}{6}}}{\left[1 + \left(\frac{0.492}{Pr}\right)^{\frac{9}{16}}\right]^{\frac{8}{27}}} \right\}^2 \tag{10}$$

$$q'' = h_{mac}(T_w - T_{spt})F + h_{mic}(T_w - T_{spt})S \tag{11}$$

$$h_{mac} = \frac{k}{D}CRe^{0.8}Pr^{0.4} \tag{12}$$

$$h_{mic} = 0.00122\left(\frac{k_f^{0.79}C_{pf}^{0.45}\rho_f^{0.49}g_f^{0.25}}{\sigma^{0.5}\mu_f^{0.29}h_{fg}^{0.24}\rho_g^{0.24}}\right)\Delta T_w^{0.24}\Delta P^{0.75} \tag{13}$$

Table 2
Reference design parameters of indefinite PRHRS.

Parameter	Value
ECT area (m^2)	20
ECT height (m)	5
ECT volume (m^3)	100 × 2
Height difference between ECT and DACT (m)	5
DACT height (m)	27.5
HX-ECT	
Length of HX-ECT (m)	2.5
Number of tubes	200 × 4
Heat transfer area of HX-ECT (m^2)	28.3 × 4
HX-IL	
Length of HX-IL (m)	2.5
Number of tubes	400 × 2
Heat transfer area of HX-IL (m^2)	56.5 × 2
HX-DACT	
Height of HX-DACT (m)	2.5
Number of tubes	800 × 2
Heat transfer area including fin effect (m^2)	1131.0 × 2

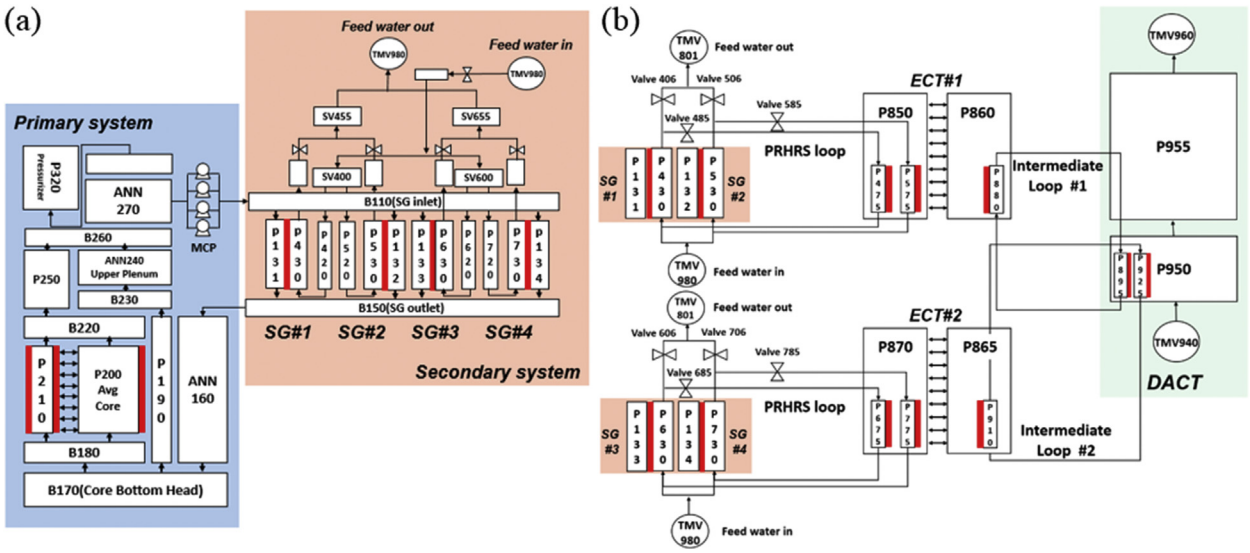

Fig. 4. Nodalization of 1D MARS-KS model: (a) SMR-IPWR; (b) indefinite PRHRS.

4. Results and discussions

To assess the feasibility of the proposed indefinite PRHRS design, it is essential to conduct transient simulations. Prior to the transient simulation, a steady-state analysis was carried out to verify the reliability of the MARS model of the SMR-IPWR. Through this steady-state simulation, we identified important design parameters, such as the coolant's mass flow rate, temperature, and pressure, to confirm the performance and condition of the reactor during normal operation. The results obtained by the MARS steady-state simulation were compared with the design parameters of the SMR-IPWR. As presented in Table 3, the MARS results are in good agreement with the design parameters, which confirms the reliability of the MARS model of the SMR-IPWR.

4.1. Feasibility assessment of indefinite PRHRS

The primary function expected from the PRHRS is to mitigate accidents by removing residual heat without the support of active safety systems. The SBO accident, which is accompanied by the unavailability of active safety systems, was selected as the reference accident scenario to assess the advantage of the indefinite PRHRS. A simulation was conducted wherein the SBO accident occurred after 1000 s of steady-state normal operation. The main coolant pumps stopped operating and the reactor was shut down owing to a trip signal indicating the low flow velocity of primary coolant. Simultaneously, the circulation of feed water stopped and the PRHRS was actuated by opening the PRHRS valves. To conservatively evaluate the accident mitigation capability of the indefinite PRHRS, it was assumed that other safety systems, except the indefinite PRHRS, were not available during the simulation.

To confirm the feasibility of the indefinite PRHRS, a long-term MARS simulation was conducted for 72 h. Fig. 5 shows the MARS simulation results for the cooling performance of each component in the indefinite PRHRS. The residual heat that was continuously generated after the reactor shutdown exponentially decreased. According to Fig. 5, the amount of heat transferred to the ECT was equal to the residual heat for 72 h, which indicates that the residual heat was successfully extracted from the reactor core to the ECT by the PRHRS. The stable establishment of the natural circulation in the PRHRS loops was also confirmed. Because of this natural circulation flow, it was possible to transfer the residual heat to the ECT. Moreover, the DACT removed a part of heat from the ECT through the air flow. In the DACT, a naturally induced air flow of 146.24 kg/s was observed. In the early stage of the accident, the amount of heat removed by the DACT gradually increased. After 6 h, the DACT exhibited an approximately constant heat removal rate. This can be explained by the change of water temperature inside the ECT. The temperature of the water stored in the ECT was elevated because the residual heat was transferred to the ECT. Because the temperature of the water stored in the ECT was elevated, the temperature difference between the water stored in the ECT and the coolant in the intermediate loop increased. Owing to this increase in the temperature difference, more heat was transferred to the DACT and removed by the air flow. The water temperature stopped increasing when it reached the saturation temperature of 100 °C, and the rate of heat removal by the DACT had a constant value from this point onward. Thus, it is reasonable to conclude that the temperature difference between the stored water and the coolant in the intermediate loop determined the rate of heat removal by the DACT. Because the residual heat decreased exponentially, the net heat consumed by the latent heat of the stored water was reduced. Thus, it was confirmed that the DACT removed most of the residual heat transferred to the ECT two days after the accident occurred.

The feasibility of the indefinite PRHRS should be evaluated from two perspectives. First, the cooling capability to remove the residual heat is assessed. Because the primary function of the PRHRS is to remove the residual heat, it is imperative to assess the cooling capability of the indefinite PRHRS. Secondly, the cooling sustainability of the indefinite PRHRS, which determines the overall grace period against the release of the fission products to the environment, is assessed. This assessment can determine the feasibility of the suggested design of the indefinite PRHRS. Based on these two viewpoints, we analyzed the various results obtained by the MARS simulation.

First, to confirm the cooling capability of the indefinite PRHRS, the change of primary coolant temperatures for 72 h after the SBO accident were investigated as shown in Fig. 6. Before 1000 s, the primary coolant temperatures at the core inlet and outlet maintained their normal operation temperature, that is, 587 and 544 K, respectively. When the SBO accident occurred, the PRHRS was actuated. The primary coolant temperature at the core inlet and outlet gradually decreased over 72 h. The decrease in the coolant temperatures implies that the residual heat was sufficiently

removed from the primary system. Moreover, this demonstrates that the indefinite PRHRS can remove the decay heat from the SMR-IPWR for 72 h.

Because the PRHRS uses the latent heat of the water stored in the ECT, the sustainability of the indefinite PRHRS is closely related to the water level inside the ECT. Fig. 7 shows the variation of the water level in the ECT. The initial water level of the ECT was 5.0 m. Because, in the early phase, the residual heat was removed by the sensible heat of the stored water, the water level was maintained at 5 m. When the temperature of the stored water reached the saturation point and started to boil, the water level started to correspondingly decrease. The reduction rate of the water level decreased over time. After 48 h, the water level of the ECT was kept approximately constant at 4.24 m, which is above the length of the HXs in the ECT (2.5 m). According to this tendency, it was reasonably concluded that the water level will keep constant for an indefinite period. Moreover, this result indicates that the indefinite PRHRS can ensure an indefinite grace period for the SMR-IPWR.

Comparative simulations were carried out to confirm the effect of the indefinite PRHRS. A case of only operating the PRHRS was compared to another case of operating the PRHRS with the DACT. Fig. 8 shows the comparison results for the change in the temperature of the primary coolant and the water level of the ECT. To compare the cooling capability of both systems, the changes of the primary coolant temperatures were compared as shown in Fig. 8(a). In both cases, the primary coolant temperatures were gradually reduced, which implies that both cases of the PRHRS only and the PRHRS with the DACT successfully extracted the residual heat from the core of the reactor. However, in the case of the PRHRS only, the primary coolant temperatures, which had decreased, gradually began to increase at 28 h. After 61 h, the primary coolant temperatures increased dramatically. In the case of the PRHRS with the DACT, the primary coolant temperatures decreased for 72 h without any increase turning point. This indicates that the cooling capability between the cases of the PRHRS only and the PRHRS with the DACT started to deviate at 28 h. The cause for the cooling capability difference was confirmed by the water level of the ECT, as shown in Fig. 8(b). In the case of the PRHRS only, the water level of the ECT steadily decreased. After 28 h, the water level was lower than the height of the HX-ECT. Finally, the stored water was completely lost at 61 h. The water level gradually decreased as the PRHRS removed the residual heat by the latent heat of the water stored in the ECT. Although the water level decreased, the PRHRS could transfer the residual heat to the ECT with the same efficiency as long as the HX-ECT was immersed in the stored water. However, as the HX began to be exposed to air, the heat transfer efficiency of the PRHRS significantly deteriorated. Thus, in the case of operating the PRHRS only, the primary coolant temperature started to increase at 28 h, when the HX-ECT was exposed to air. As the water level of the ECT continued to decrease, the cooling efficiency of the PRHRS deteriorated. Finally, the stored water was lost and the PRHRS failed to remove the residual heat, as was confirmed by the sudden increase of the primary coolant temperature. In contrast, in the case of operating the PRHRS with the DACT, the water level was

Table 3
Comparison between operating condition of SMR-IPWR and MARS simulation.

Parameter	Design value	MARS result	Rel. Error (%)
Thermal power (MW)	330	330.01	0.3
Operating pressure (MPa)	15	15.13	0.87
Core inlet temperature (K)	546.04	544.8	0.2
Core outlet temperature (K)	588.08	586.9	0.2
Temperature difference (K)	42.04	42.1	0.14
Feed water inlet temperature (K)	430.88	430.69	0.04
SG pressure (MPa)	4.42	4.41	0.23

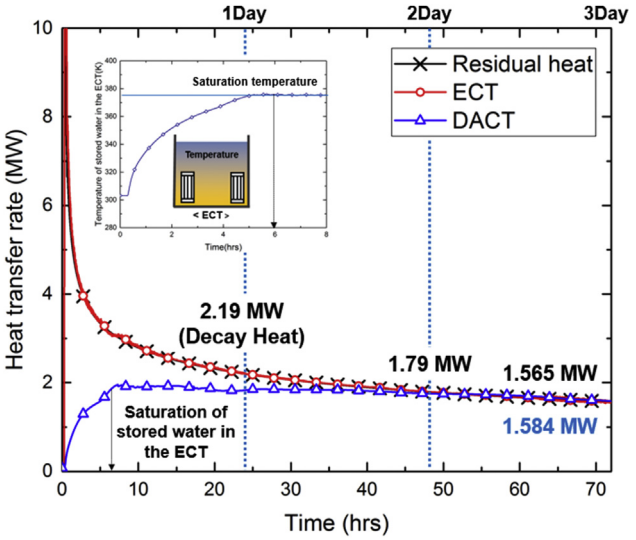

Fig. 5. Residual heat and heat transfer rate of ECT and DACT.

maintained over the height of the HX-ECT. Because the exposure of the HX was prevented, the PRHRS with the DACT successfully removed the residual heat for 72 h. According to the results, the grace period of the SMR-IPWR can be extended indefinitely by the indefinite PRHRS with the same ECT volume.

4.2. Parametric analysis of environmental temperature

The environmental temperature is the most important parameter affecting the cooling performance of the indefinite PRHRS. To evaluate the effect of the environmental temperature on the indefinite PRHRS, a parametric analysis was conducted using MARS-KS. Simulations were carried out with different environmental temperatures from 20 °C to 60 °C. Fig. 9 presents the change of the ECT water level at various environmental temperatures. As the environmental temperature increased, the amount of water stored in the ECT was reduced. In the cases with 20 °C–40 °C, the exposure of the HXs was prevented for 72 h. In the cases with 50 °C and 60 °C, the water levels were reduced to 2.01 m and 1.31 m, respectively, which are lower than the height of the HXs. This indicates that the effect of delaying the loss of stored water by the DACT deteriorated

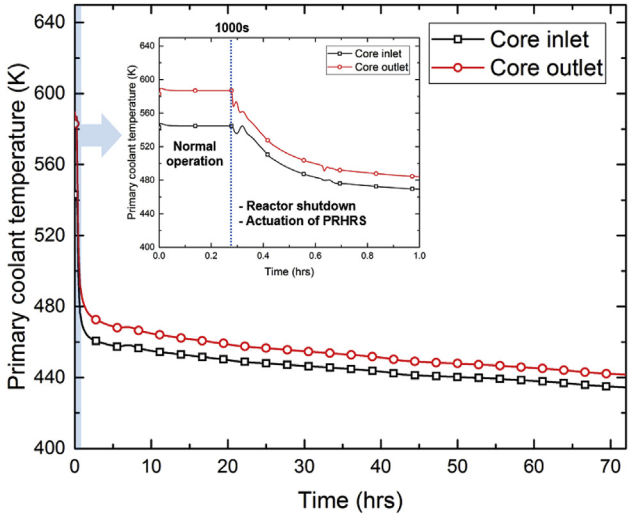

Fig. 6. Change of primary coolant temperatures at core inlet and outlet.

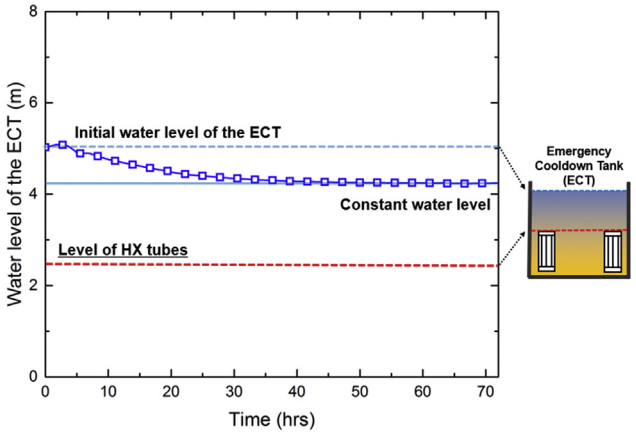

Fig. 7. Change of water level inside ECT (the top part of the heat exchanger is located at 2.5 m, as indicated by the red line.). (For interpretation of the references to colour in this figure legend, the reader is referred to the Web version of this article.)

owing to the increase of the environmental temperature. However, even under severe environmental conditions with 60 °C, the indefinite PRHRS still ensured a more extended grace period compared with the PRHRS.

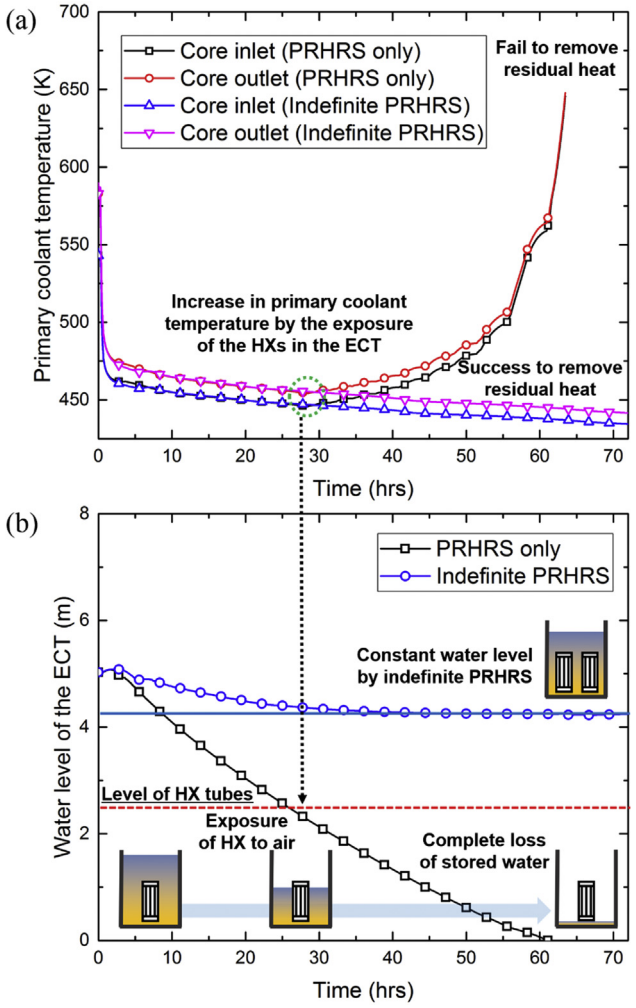

Fig. 8. Comparison of both cases of PRHRS and indefinite PRHRS: (a) primary temperature coolant; (b) water level of ECT.

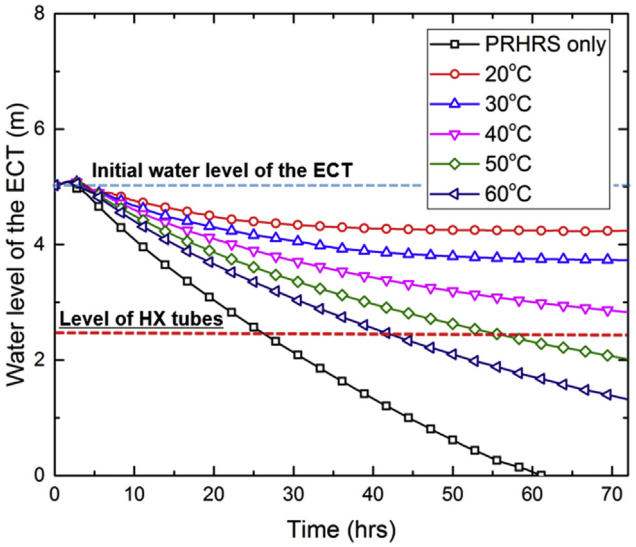

Fig. 9. Change of ECT water level at various environmental temperatures.

Fig. 10 shows the change of the primary coolant temperature at various environmental temperatures. In all cases, the primary coolant temperatures decreased in a similar manner until the HX was exposed. This implies that the change of the environmental temperature does not directly affect the cooling performance of the PRHRS. Before the HX was exposed to air, the PRHRS maintained its cooling efficiency regardless of the environmental temperature. The point where the primary coolant temperature started to increase was delayed by the DACT. This delay effect was caused by the environmental temperature. When the environmental temperature changed from 20 °C to 40 °C, the primary coolant was continuously decreased for 72 h by the indefinite PRHRS. In the cases of 50 °C and 60 °C, the increment of the primary coolant temperature occurred at 61 h and 47 h, which is a considerable delay compared with the case of the PRHRS only.

We confirmed that the environmental temperature increase deteriorated the cooling performance of the DACT. This deterioration can be explained by the temperature gradient. According to Fig. 11, the average coolant temperatures in the intermediate loop

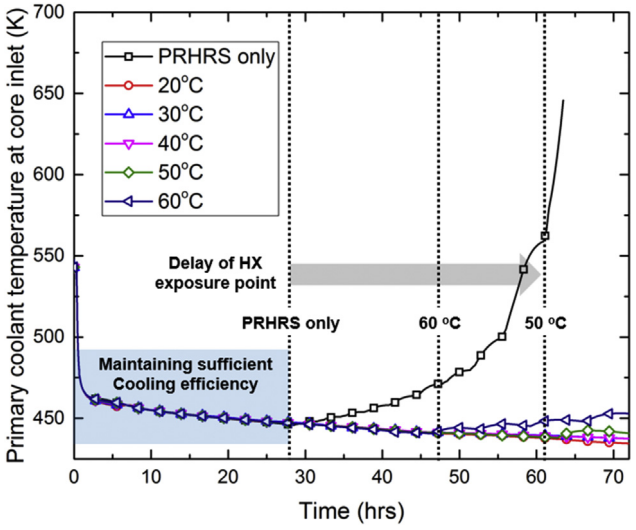

Fig. 10. The change of the primary coolant temperature in the cases with various environmental temperatures.

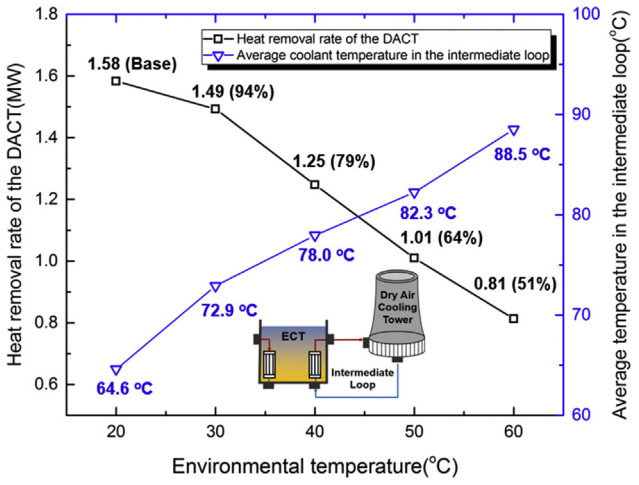

Fig. 11. Heat transfer rate of DACT and average temperature in intermediate loop at various environmental temperatures.

increased with the environmental temperature. At the HX-IL, the heat from the water stored in the ECT was transferred to the coolant in the intermediate loop by the temperature gradient between the two fluids. The hot coolant also transferred the heat to the environmental air by the temperature gradient at the HX-DACT. However, as the environmental temperature increased, the temperature gradient between the hot coolant and the air decreased. Owing to the reduced temperature gradient, the temperature of the coolant became greater than that of the base case after passing through the DACT. This relatively high coolant temperature also lowered the temperature gradient at the HX-IL. Thus, the amount of heat transferred from the ECT was diminished. The environmental temperature increase deteriorated the mitigating effect on the loss of water stored in the ECT.

5. Conclusions

This study presented an advanced PRHRS concept, namely, the indefinite PRHRS, which is designed to ensure an indefinite grace period by incorporating the DACT to the PRHRS. We assessed the feasibility of the indefinite PRHRS from two perspectives using MARS-KS: the cooling capability and sustainability of the indefinite PRHRS. Additionally, a parametric analysis was conducted to confirm the effect of the environmental temperature on the indefinite PRHRS. The major conclusions drawn from this study are as follows:

(1) The indefinite PRHRS successfully removed the residual heat of the reference SMR-IPWR for 72 h. Stable natural circulation flows, which are essential for operating the system, were established in the PRHRS loop, intermediate loop, and DACT.
(2) The DACT removed the heat from the water stored in the ECT by the naturally driven air flow inside the DACT. As the residual heat exponentially decreased, the DACT removed all of the residual heat transferred to the ECT two days after the reactor shutdown. The water level in the ECT was kept constant at 4.24 m, which is higher than the height of the HXs in the ECT. Thus, it was confirmed that the indefinite PRHRS can ensure an indefinite grace period.
(3) As the environmental temperature increased, the sustainability of the indefinite PRHRS declined. However, even under the extreme condition of 60 °C, the sustainability of the indefinite PRHRS was extended compared with the case of the PRHRS only.
(4) The variation on the cooling performance of the DACT did not directly affect the cooling efficiency of the PRHRS until the HX was exposed. This affected the cooling sustainability of the indefinite PRHRS. Owing to these characteristics, the indefinite PRHRS can ensure at least the same grace period as the PRHRS only, even under extreme environmental conditions.

In conclusion, through this study, the feasibility of indefinite PRHRS in terms of thermal-hydraulics was confirmed. However, economical and physical feasibility still remain to be resolved. Installing a PRHRS with a much larger ECT volume could be more cost effective but, at the same time, containment may have to be sized up to incorporate the larger ECT. So the overall evaluation of the economy needs to be studied in future work. Resolving the physical difficulty of installing the DACT at higher elevation than the ECT also remains unresolved for on-ground reactors. Nevertheless, the indefinite PRHRS is expected to be applied for the SMR with underground siting as most of the component lies underground. Furthermore, the concept of indefinite PRHRS can be applied to the reactor with an indirect dry air-cooled condenser using the air cooling tower as an ultimate heat sink. The air cooling tower for the condenser can work as the DACT for the indefinite PRHRS during the accident condition. It is expected to enhance the availability of the cooling tower even during the accident scenarios.

Declaration of competing interest

We declare that the submitted work has no conflict of interest with any relevant research institutes, academics, or industries.

Acknowledgements

This study was supported by the National Research Foundation of Korea (NRF), funded by the Ministry of Science, ICT, and Future Planning, Republic of Korea (No. NRF-2016R1A5A1013919) and the Human Resources Program in Energy Technology of the Korea Institute of Energy Technology Evaluation and Planning (KETEP) granted financial resource from the Ministry of Trade, Industry & Energy, Republic of Korea (No. 20184030201970)

Appendix A. Supplementary data

Supplementary data to this article can be found online at https://doi.org/10.1016/j.net.2019.11.003.

References

[1] J. Vujic, R.M. Bergmann, R. Skoda, M. Miletic, Small modular reactors: Simpler, safer, cheaper? Energy 45 (2012) 288–295.
[2] A. Lokhov, R. Cameron, V. Sozoniuk, OECD/NEA study on the economics and market of small reactors, Nucl. Eng. Technol. 45 (2013) 701–706.
[3] M.V.I. Fukami, A. Santecchia, CAREM project: innovative small PWR, Prog. Nucl. Energy 37 (2000) 265–270.
[4] K.H. Bae, H.C. Kim, M.H. Chang, S.K. Sim, Safety evaluation of the inherent and passive safety features of the smart design, Ann. Nucl. Energy 28 (2001) 333–349.
[5] M.D. Carelli, L.E. Conway, L. Oriani, B. Petrovic, C.V. Lombardi, M.E. Ricotti, A.C.O. Barroso, J.M. Collado, L. Cinotti, N.E. Todreas, D. Grgic, M.M. Moraes, R.D. Boroughs, H. Ninokata, D.T. Ingersoll, F. Oriolo, The design and safety features of the IRIS reactor, Nucl. Eng. Des. 230 (2004) 151–167.
[6] K. Shirvan, P. Hejzlar, M.S. Kazimi, The design of a compact integral medium size PWR, Nucl. Eng. Des. 243 (2012) 393–403.
[7] G.H. Seo, D. Shin, H.H. Son, Y. Kim, J.I. Lee, S.J. Kim, Preliminary Study of Conceptual Design of the ATOM Safety System, Nuclear Reactor Thermal Hydraulics, 2017. Xian China, September 3-8.
[8] X.H. Nguyen, C. Kim, Y. Kim, An advanced core design for a soluble-boron-free small modular reactor ATOM with centrally-shielded burnable absorber, Nucl. Eng. Technol. 51 (2019) 369–376.
[9] H. Ninokata, A comparative overview of thermal hydraulic characteristics of

integrated primary system nuclear reactors, Nucl. Eng. Technol. 38 (2006) 33–44.
[10] N. Jiang, M. Peng, T. Cong, Simulation analysis of an open natural circulation for the passive residual heat removal in IPWR, Ann. Nucl. Energy 117 (2018) 223–233.
[11] P.E. Juhn, J. Kupitz, J. Cleveland, B. Cho, R.B. Lyon, IAEA activities on passive safety systems and overview of international development, Nucl. Eng. Des. 201 (2000) 41–59.
[12] G.L. Xia, M. Peng, X. Du, Calculation analysis on the natural circulation of a passive residual heat removal system for IPWR, Ann. Nucl. Energy 72 (2014) 189–197.
[13] H.N. Butt, M. Ilyas, M. Ahmad, F. Aydogan, Assessment of passive safety system of a small modular reactor (SMR), Ann. Nucl. Energy 98 (2016) 191–199.
[14] H.S. Park, K.Y. Choi, S. Cho, S.J. Yi, C.K. Park, M.K. Chung, Experiments on the performance sensitivity of the passive residual heat removal system of an advanced integral type reactor, Nucl. Eng. Technol. 41 (2009) 53–62.
[15] B.Y. Min, H.S. Park, Y.C. Shin, S.J. Yi, Experimental verification on the integrity and performance of the passive residual heat removal system for a SMART design with VISTA-ITL, Ann. Nucl. Energy 71 (2014) 118–124.
[16] Y. Zhang, S. Qiu, G. Su, W. Tian, Design and transient analyses of emergency passive residual heat removal system of CPR1000, Nucl. Eng. Des. 242 (2012) 247–256.
[17] M. Wang, H. Zhao, Y. Zhang, G. Su, W.X. Tian, S. Qiu, Research on the designed emergency passive residual heat removal system during the station blackout scenario for CPR1000, Ann. Nucl. Energy 45 (2012) 86–93.
[18] T. Suzuki, Deconstructing the zero-risk mindset: the lessons and future responsibilities for a post-Fukushima nuclear Japan, Bull. At. Sci. 67 (2011) 9–18.
[19] S.H. Chang, S.H. Kim, J.Y. Choi, Design of integrated passive safety system (IPSS) for ultimate passive safety of nuclear power plants, Nucl. Eng. Des. 260 (2013) 104–120.
[20] Y. Zhang, S. Qiu, G. Su, W. Tian, Design and transient analyses of emergency passive residual heat removal system of CPR1000. Part I: air cooling condition, Prog. Nucl. Energy 53 (2011) 471–479.
[21] M. Wang, S. Qiu, W. Tian, G. Su, Y. Zhang, The comparison of designed water-cooled and air-cooled passive residual heat removal system for 300 MW nuclear power plant during the feed-water line break scenario, Ann. Nucl. Energy 57 (2013) 164–172.
[22] M.J. Kim, J.H. Moon, Y. Bae, Y.I. Kim, H.J. Lee, Feasibility test of the concept of long-term passive cooling system of emergency cooldown tank, Ann. Nucl. Energy 80 (2015) 403–408.
[23] X. Lv, M. Peng, X. Yuan, G. Xia, Design and analysis of a new passive residual heat removal system, Nucl. Eng. Des. 303 (2016) 192–202.
[24] Z.Y. Guo, X.B. Liu, W.Q. Tao, R.K. Shah, Effectiveness-thermal resistance method for heat exchanger design and analysis, Int. J. Heat Mass Transf. 53 (2010) 2877–2884.
[25] H. Ayhan, C.N. Sokmen, Investigation of passive residual heat removal system for VVERs: effects of finned type heat exchanger tubes, Appl. Therm. Eng. 108 (2016) 466–474.
[26] Thermal-Hydraulic Safety System Research Department, MARS CODE MANUAL VOLUME V: Models and Correlations, Korea Atomic Energy Research Institute, 2009. KAERI/TR-3872/2004.
[27] S.S. Jeon, S.J. Hong, J.Y. Park, K.W. Seul, G.C. Park, Assessment of horizontal in-tube condensation models using MARS code. Part I: Stratified flow condensation, Nucl. Eng. Des. 254 (2013) 254–265.
[28] X.G. Yu, H.S. Park, Y.S. Kim, K.H. Kang, S. Cho, K.Y. Choi, Systematic analysis of a station blackout scenario for APR1400 with test facility ATLAS and MARS code from scaling viewpoint, Nucl. Eng. Des. 259 (2013) 205–220.
[29] Thermal-Hydraulic Safety System Research Department, MARS CODE MANUAL VOLUME I: Code Structure, System Models, and Solution Methods, Korea Atomic Energy Research Institute, 2009. KAERI/TR-2812/2004.
[30] Thermal-Hydraulic Safety System Research Department, MARS CODE MANUAL VOLUME II: Input Requirements, Korea Atomic Energy Research Institute, 2009. KAERI/TR-2811/2004.
[31] A. Hedayat, Simulation and transient analyses of a complete passive heat removal system in a downward cooling pool-type material testing reactor against a complete station blackout and long-term natural convection mode using RELAP5/3.2 code, Nucl. Eng. Technol. 49 (2017) 953–967.
[32] S.H. Kang, S.W. Lee, H.G. Kang, Performance analysis of the passive safety features of iPOWER under Fukushima-like accident conditions, Nucl. Eng. Technol. 51 (2019) 676–682.
[33] S.W. Churchill, H.H.S. Chu, Correlating equations for laminar and turbulent free convection from a vertical plate, Int. J. Heat Mass Transf. 18 (1975) 1323–1329.
[34] A.Y. Inayatov, Correlation of data on heat transfer flow parallel to tube bundles at relative tube pitches of $1.1<s/d<1.6$, Heat Transf. Sov. Res. 7 (1975) 84–88.
[35] J.C. Chen, Correlation for boiling heat transfer to saturated fluids in convective flow, Ind. Eng. Chem. Process Des. Dev. 5 (1966) 322–329.
[36] F.W. Dittus, L.M.K. Boelter, Heat transfer in automobile radiators of the tubular type, Int. Commun. Heat Mass Transf. 12 (1985) 3–22.